Geochemistry International, Vol. 41, No. 10, 2003, pp. 947–958. Translated from Geokhimiya, No. 10, 2003, pp. 1036–1047.

Effect of Water on the Melting Curves of Minerals: The Olivine–Melt Equilibrium

A. P. Maksimov

Institute of Volcanic Geology and Geochemistry, Far East Division, Russian Academy of Sciences, bul'v. Piipa 9, Petropavlosk-Kamchatskii, 683006 Russia

e-mail: a_max@pisem.net

Received December 7, 2001

Abstract—The behavior of the melting curves of anhydrous silicates in the presence of water is examined in T–C_w and P–T diagrams. It is demonstrated that the effect of water on the melting temperatures of minerals can be explained with the use of the constants of the melting reactions under anhydrous conditions, with melt components assumed to be oxides recalculated to one cation. The water effect is thereby taken into account through a decrease in the fractions of melt components in compliance with the ideal solution model. The general form of the equation for the dependence of the melting temperature on the water concentration in melt satisfactorily reproduces the configurations of the liquidus curves. The example of the olivine–melt equilibrium is employed to demonstrate that the ideal model is able to quantitatively explain the extent of the melting temperature decrease when water is added. In order to adequately describe the experimental data, it is proposed to use a formal parameter: the effective water concentration, which takes into account the presence of the molecular and hydroxyl modes of water occurrence in the melt.

INTRODUCTION

The good water solubility in silicate melts predetermines its crucial effect on the stability of magmatic minerals. To calculate the physicochemical parameters of natural magmatic melts that bear even relatively low water concentrations, techniques are required that make it possible to take into account the effect of water on the decrease in the melting temperatures. A rigorous solution of this problem should be based on the knowledge of melt structures, the thermodynamic constants of melt components, and the interaction parameters of these components. Since information of this kind is still very scarce, the researcher is left with the possibility to rely on practically exclusively empirical and semiempirical approaches based on a variety of models for silicate melts.

From the viewpoint of thermodynamics, there are two principal approaches to the problem of calculating magmatic equilibria: (1) selection of thermodynamic functions of the dissolution reactions and the activity coefficients of melt components, usually within the framework of the regular solution theory [1]; and (2) determination of the equilibrium constants of mineral–melt reactions [2–5]. In the latter situation, the activities of melt components are taken to be equal to their mole fractions, although the form of the equilibrium constant function makes it possible to take into account the effect of the melt composition [2]. Whatever the differences in the thermodynamic formalism of the two approaches, they share the statistical treatment of experimental data with the aim of determining the optimal values of the parameters and constants that can best fit the model proposed.

The significance of the effect of water on magmatic equilibria is reflected in the diversity of models proposed to describe its interactions with melts, techniques for calculating the water solubility, and approaches to estimating the decrease in the melting temperatures [1, 6–16, and others].

A simple method enabling the evaluation of the water effect in the theoretical modeling of magma crystallization was developed by Al'meev and Ariskin [16] and involves the assumption of a proportional effect of the water percent concentration in the melt on the decrease of the liquidus temperature of a given mineral. Proceeding from experimental data, these researchers calculated average correction coefficients for olivine, ortho- and clinopyroxene, and plagioclase for certain pressures over the interval of 1 to 10 kbar. The effect of water was evaluated by the equation

$$T_w^i = T_0^i - \lambda_{C_w}^i, \quad (1)$$

where T_w^i and T_0^i are the liquidus temperatures of mineral i under aqueous and anhydrous conditions, respectively; λ^i is the correction coefficient; and C_w is water wt % in the melt.

As is demonstrated below, there is a natural and simple approach that makes it possible to roughly reproduce the effect of water on the configuration of the liquidus lines of the main rock-forming minerals and

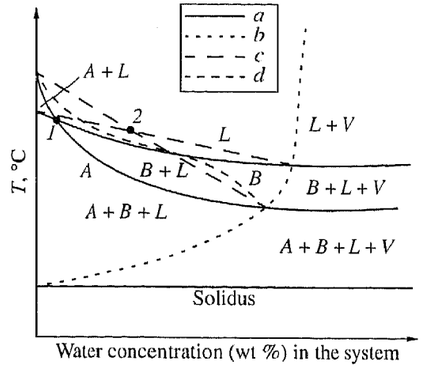

Fig. 1. Schematic T–H_2O section of a diagram for the crystallization of the rock–H_2O system at P_{total} = const. (*a*) Melting curves of anhydrous silicate minerals (*A*, *B*); (*b*) curve of system saturation with water; (*c*) melting curves of minerals in the situation with the proportional water effect on the melting temperature according to the model [16]; (*d*) a more complicated variant of the melting curve of phase *A*. *L*—melt, *V*—fluid, *1* and *2* are the intersection points of the melting curves.

yields a quantitative estimate of this effect for the olivine–melt equilibrium.

EFFECT OF WATER ON THE LIQUIDUS LINES OF MINERALS

Now consider the principal features of the effect of water on the melting temperatures of minerals and the morphology of the melting lines in diagrams of two types: (1) temperature versus water concentration in the system (T–C_w) under a constant total pressure (P) and (2) total pressure versus temperature (P–T) at a given water concentration in the system. A schematic diagram of the first type is presented in Fig. 1, and analogous plots for the system andesite–H_2O were published in [17]. As examples of diagrams of the other type, Figs. 2a and 2b show P–T plots for andesite crystallization under conditions of water saturation and generalized P–T plots of the olivine tholeiite liquidus at different water concentrations in the melt from [17, 18]. These plots demonstrate the main regularities in the changes in the melting temperatures of anhydrous silicate minerals when water is added to the system.

T–C_w (P = const) Diagram, Fig. 1

(1) An increase in the water concentration in the system continuously decreases the liquidus temperature until the melt becomes saturated in water; further water addition does not bring about any changes in the melting temperature, a phenomenon reflecting the constancy of the water concentration in the melt.

(2) The strongest decrease in the liquidus temperature (the highest absolute values of dT_L/dC_w) is attained in the region of low water concentrations (the melt contains a few water percent added to it). As water-saturated conditions are approached, the liquidus lines usually become inclined more gently. However, as follows from the model [16], the proportional effect of water on T_L should result in liquidus lines in the form of straight lines connecting the temperatures of the dry and water-saturated liquidi (Fig. 1, line *c*).

Sometimes the behaviors of T–C_w liquidus lines are more complicated and have inflections in the undersaturation region. One of the possible situations is shown in Fig. 1 as line *d*.

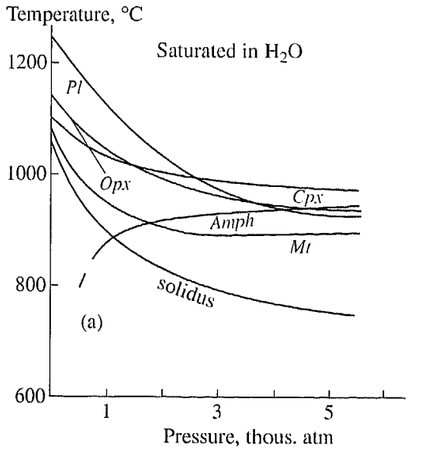

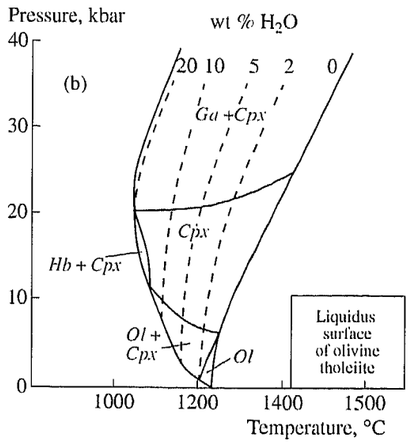

Fig. 2. (a) P–T diagram of andesite crystallization under water-saturation conditions [17]; (b) generalized liquidus P–T curves and stability fields of phases on the liquidus for an olivine tholeiite composition at different water concentrations [19]. *Pl*—plagioclase, *Ol*—olivine, *Cpx*—clinopyroxene, *Opx*—orthopyroxene, *Ga*—garnet, *Hb*—hornblende, *Amph*—amphibole, *Mt*—magnetite.

(3) The degree to which the liquidus temperature diminishes with water addition usually systematically increases in the succession $Ol \longrightarrow OPx \longrightarrow CPx \longrightarrow Pl$. This regularity is quite obvious from Table 1, obtained in [16] by statistical treatment of experimental results for water-saturation conditions. A consequence of this is a change in the liquidus phases and a different crystallization order of minerals at different water concentrations in the system. This is of paramount importance for the analysis of the crystallization conditions of natural magmas [17] and for interpreting genetic relations between magmas and the evolutionary trends of melts. As can be seen from Fig. 1, the position of the intersection points of the stability lines of minerals in a melt can be notably different from those obtained by means of rectilinear interpolations of the melting temperatures in compliance with the model in [16] (point *1* $\longrightarrow$ point *2*).

P–T (C_w = const) Diagrams, Fig. 2

(4) Water pressure (P_w) exerts the greatest effect on the melting lines in the region of low pressures (analogously to the region of low concentrations in the T–C_w diagram), which is also in good agreement with the data in Table 1.

(5) The P–T melting curves show temperature minima even under water-saturation conditions, and an increase in the water concentration shifts the minima toward higher pressures. The occurrence of minima in the P–T curves is usually explained by a decrease in the molar volume of water under high pressures [6, 19].

(6) A pressure increase also brings about intersections between the stability curves of phases in the P–T diagrams, which, in turn, results in modified successions of their crystallization.

(7) The slopes of the P–T curves at certain water concentrations $(dT_L/dP)_{C_w}$ in the undersaturated region are prone to decrease with increasing H_2O concentration (Fig. 2b, lines for 0 to 10% H_2O).

The effects listed above are mostly of universal character and are characteristic of normal types of silicate systems. Hence, a model for describing the effect of water on the melting of silicates should explain the character and magnitudes of these effects.

EFFECT OF MELT DILUTION WITH WATER: GENERAL REGULARITIES

The mechanisms of water interaction with melts and effect of water on the melt structures, as well as the thermodynamic properties of melts, are still poorly understood. As was mentioned above, a series of approaches was proposed to calculate the melting temperatures of minerals as functions of water contents in the melts. Below we will demonstrate the possibility of reproducing the effect of water on the configuration of the liquidus curves of anhydrous minerals and on the decrease in the melting temperature by the simplest means: through the diluting effect of water particles on melt composition according to the ideal solution model. Burnham [10] pointed out that the effect of water on a decrease in the melting temperatures is so significant that it cannot be accounted for only by the effect of dilution of the components of a "dry" melt. However, the effect itself seems to have been evaluated based on the notion that water was dissolved in the molecular mode, while water dissolution in the form of OH groups dramatically increases the dilution degree.

Table 1. Coefficients λ^i (°C/1% H_2O) in Eq. (1) for the main rock-forming minerals depending on pressure (from [16])

P, kbar	λ^{Ol}	λ^{OPx}	λ^{Aug}	λ^{Pl}
1	17.9 ± 6.0	22.4 ± 3.4	34.3 ± 7.1	59.6 ± 7.8
2	18.7 ± 2.9	22.3 ± 1.2	24.8 ± 2.2	49.9 ± 4.2
2.5			23.7 ± 3.9	47.6 ± 1.0
3		18.3		43.1 ± 1.5
4				38.3 ± 1.6
5	10.2 ± 5.5		15.5 ± 3.3	38.1 ± 3.1
6.9				37.8 ± 0.6
7.5	5.1 ± 3.7	12.5 ± 2.2	14.5 ± 1.6	
10	1.3 ± 0.7	9.3 ± 1.0	10.5 ± 1.1	

In order to calculate the effect of water on the temperatures of equilibria between silicate minerals and melts, one can use equilibrium constants for melting reactions under dry conditions, with the water effect taken into account through a decrease in the mole fractions of melt components (which are assumed to be one cation per formula unit).

The crystallization equation for an end member M contained in a solid phase S can be written in a general form as

$$aA^L + bB^L + \ldots + kK^L = M^S, \qquad (2)$$

where A^L, B^L, …, K^L are one-cation oxides in melt L; and a, b, …, k are the stoichiometric coefficients. The activity of component i in an ideal solution (melt) is equal to its mole fraction, $a_i = X_i$. Then, the equilibrium constant of reaction (2) is expressed as

$$\ln K = \ln \frac{X_M^S}{(X_A^L)^a (X_B^L)^b \ldots (X_K^L)^k}. \qquad (3)$$

According to the conventional approach, the temperature (K) and pressure (bar) function of the equilibrium constant of a reaction can be written as

$$\ln K = \frac{A}{T} + B + C\frac{P-1}{T}, \qquad (4)$$

where A, B, and C are constants.[1] This dependence can be considered valid for equilibrium constants in both water-bearing (K_w) and dry (K_0) melts, because it describes the same equilibrium (2) in both situations.

The mole fractions of component i in dry $(X_i^L)_0$ and water-bearing $(X_i^L)_w$ melts can be expressed as

$$(X_i^L)_0 = n_i^L/n_0 \text{ and } (X_i^L)_w = n_i^L/(n_0 + n_w), \quad (5)$$

where n_i^L is the number of moles (cations) of component i in the melt, n_0 is the overall number of cations in 100 g of the dry melt, and n_w is the number of water particles formed during water dissolution in the melt. It follows that

$$K_w/K_0 = (1 + n_w/n_0)^m, \quad (6)$$

where $m = a + b + \ldots + k$ is the number of particles produced during the melting of the mineral by reaction (2).

The temperature of equilibrium (2) in the water-bearing melt from Eq. (4) is

$$T = \frac{A + C(P-1)}{\ln K_w - B}. \quad (7)$$

Then, from Eqs. (6) and (7),

$$T = \frac{A + C(P-1)}{\ln K_0 - B + m\ln(1 + n_w/n_0)}. \quad (8)$$

The number of water particles contained in 100 g of the dry melt is related to the water concentration (C_w) as

$$n_w = \frac{100C_w}{(100 - C_w)W}, \quad (9)$$

where W is the gram formula weight of the water particles (9.01 for hydroxyl and 18.02 for molecular water).[2]

The equilibrium temperature in water-bearing melts can be determined from the equation

$$T = \frac{A + C(P-1)}{\ln K_0 - B + m\ln[1 + 100C_w/(100 - C_w)Wn_0]}, \quad (10)$$

where A, B, and C are constants; P is pressure (bar); K_0 is the equilibrium constant of the crystallization reaction at $P = 1$ bar; m is the number of particles produced in the process of mineral melting; C_w is the water concentration in the melt (wt %); W is the molecular weight of water particles; and n_0 is the total number of cations contained in 100 g of the dry melt.

[1] This dependence implies that (1) the heat capacity of the reaction $\Delta C_p = 0$, so that the enthalpy ΔH_0 and entropy ΔS_0 of the reaction do not depend on temperature, and (2) the volume difference of the reaction ΔV_0 is also temperature and pressure independent, i.e., $A = -\Delta H_0/R$, $B = \Delta S_0/R$, and $C = -\Delta V_0/R$.

[2] For simplicity, it is assumed in expression (9) that the melt contains water particles of only one type. The effect of different dissolved water speciation on the liquidus curves is discussed below.

The mathematical analysis of Eqs. (8) and (10) makes it possible to explain the aforementioned regularities in the behavior of the melting curves.

T–C_w Diagrams

(1) The dependence expressed by Eq. (8) indicates that the first-order derivative $(\partial T/\partial n_w)_P$ is always smaller than zero. The $(\partial T/\partial C_w)_P$ derivative behaves analogously, because n_w and C_w increase simultaneously. This implies that the liquidus temperature in isobaric sections continuously decreases with increasing n_w and C_w until it attains the highest possible water pressure in the melt at this temperature.

(2) Since the second-order derivative $(\partial^2 T/\partial n_w^2)_P > 0$, the liquidus line in a T–n_w diagram is concave. This fact reflects the maximum influence of water in the region of its low concentrations. Because the same derivative at a constant pressure does not reverse its sign, the melting curve has no minimum and becomes sloped more gently closer to the saturation curve, analogously to curves a in Fig. 1. However, the complex character of the dependence of the speciation of dissolved water on its concentration [11, 12] predetermines a more complicated form of the $(\partial^2 T/\partial C_w^2)_P$ derivative, and the behavior of the T–C_w liquidus curves is, in the general case, different. For instance, they can possess inflection points, similarly to curve d in Fig. 1.

(3) It can also be seen from Eq. (8) that the effect of water is enhanced with an increasing coefficient m, i.e., with an increasing number of particles produced during the melting of the mineral. At the chosen scheme for the melting reaction, when the melt components are assumed to be single-cation oxides, the temperature decrease caused by water addition is greater for minerals of complex composition. The crystallization of common magmatic minerals can be expressed by the following reactions.

Olivine:	$MgO + 0.5SiO_2 = MgSi_{0.5}O_2$	$m = 1.5$
Orthopyroxene:	$MgO + SiO_2 = MgSiO_3$	$m = 2$
Clinopyroxene:	$0.5MgO + 0.5CaO + SiO_2 = Ca_{0.5}Mg_{0.5}SiO_3$	$m = 2$
Plagioclase:	$CaO + 2AlO_{1.5} + 2SiO_2 = CaAl_2Si_2O_8$	$m = 5$
	$NaO_{0.5} + AlO_{1.5} + 3SiO_2 = NaAlSi_3O_8$	$m = 5$

As a first approximation, this simplified approach enables explaining the enhancement of the water effect on the melting of minerals in the succession olivine → pyroxenes → plagioclase. However, the actual situation is much more complicated. This is obvious from, for example, the more significant decrease in the anorthite melting temperature as compared with that of albite in the presence of water. To explain this fact, an alternative reaction can be proposed for albite melting:

$$NaAlO_2 + 3SiO_2 = NaAlSi_3O_8 \quad m = 4.$$

Here, the dilution effect of water on the reaction constant for albite melting is weaker than for the reaction of anorthite melting.

Generally, an increase in the melt polymerization degree is coupled with a complication of its structural units and, accordingly, complication of the interpretation scheme for the melting of minerals. For example, water notably suppresses the melting temperature of quartz, although there is no reason to expect this judging from the simple reaction

$$\underset{\text{melt}}{SiO_2} = \underset{\text{quartz}}{SiO_2}, \quad m = 1.$$

However, here one should pay attention to constant A in Eq. (10), namely, to the following features of this equation.

(4) The effect of water on the melting curves of minerals should be greater, the lower is A, i.e., the lower the absolute value of the melting enthalpy ΔH_0 of the mineral. The melting enthalpy of quartz is much smaller than that of other rock-forming minerals. For example, the melting enthalpy of diopside $CaMgSi_2O_6$ and albite $NaAlSi_3O_8$ is 18.5 and 13.6 kcal/mol, respectively [20], while that of quartz is 2.04 kcal/mol [21]. Because of this, the same water concentration in a melt should bring about a more significant decrease in the melting temperature of quartz than those of other rock-forming minerals.

P–T Diagrams

Pressure affects the melting temperature in two manners: (1) in the H_2O-saturated region, it suppresses T_L through an increase in water solubility [an increase in the $\ln(1 + n_w/n_0)$ term in Eq. (8)], and (2) an increase in the total pressure increases the term $C(P - 1)$ and, thus, increases T_L, similarly to the situation of water-free systems. Thus, the resultant effect of pressure depends on the relations between the two effects.

(5) Under low total pressures in the water-saturated region, the liquidus temperature is decreased most significantly, because these conditions correspond to the dissolution of the very first water portions and the term $\ln(1 + n_w/n_0)$ in Eq. (8) increases most sharply (its first-order derivative is greater than and second-order derivative smaller than zero).

(6) At the same time, an increase in water content in the melt (n_w) results in progressively smaller variation in this term. Correspondingly, the comparative significance of the term $C(P - 1)$, i.e., the volume difference of the reaction, increases. When the pressure is high enough, an increase in the water concentration of the melt is counterbalanced by the effect of the volume difference in the "dry" melting reaction. This pressure corresponds to a minimum melting temperature, and a further pressure increase results in an increase in the liquidus temperature. If the water content in the system is limited, an analogous increase occurs after all the water is dissolved, and the minimum is situated in the P–T saturation curve for this amount of water. This explanation of the existence of a minimum in the P–T curve of the water-saturated liquidus does not require a change in the molar volumes of the compounds participating in the reaction, for example, the molar volume of dissolved water (which is not explicitly involved in the reaction). However, the contributions of the two proposed mechanisms responsible for a minimum in the P–T liquidus curves should be evaluated quantitatively.

(7) The relative behavior of various anhydrous phases in P–T diagrams for melting curves should be determined (at constant other parameters, for example, a constant composition of the melt) by two parameters in Eqs. (8) or (10): m and C (or ΔV_0). A phase whose melting reaction produces the greatest number of particles should be characterized by the most strongly pronounced decrease in the liquidus temperature. At the same time, C exerts the opposite effect. The relative contributions of these parameters are different for different phases under different pressures. For example, the values of m for forsterite and diopside are 1.5 and 2, and their ΔV_0 are 0.019 and 0.046 g/cm^3, respectively. Accordingly, under low and moderate pressures in water-saturated environments, a pressure increase brings about a smaller decrease in the melting temperature for olivine than for clinopyroxene, whereas under high pressures clinopyroxene appears in place of olivine as a liquidus phase in normal types of basalts (Fig. 2b). It should be mentioned that the volume difference of the melting reaction (and, correspondingly, the C coefficient) should also be taken into account under high pressures.

(8) A decrease in the slope of the P–T liquidus curves, more precisely, the value of $(dT_L/dP)_{C_w}$, with increasing water concentration is explained by a decrease in the value of

$$\frac{C}{\ln K_0 - B + m\ln[1 + 100C_w/(100 - C_w)Wn_0]}$$

with increasing C_w.

Hence, the general form of Eqs. (8) and (10) makes it possible to qualitatively explain the aforementioned morphological features of the melting curves of anhydrous silicates in the presence of water. Now consider the temperature effect of the dilution of melt components with water.

EFFECT OF MELT DILUTION WITH WATER: QUANTITATIVE CHARACTERIZATION OF THE OLIVINE–MELT EQUILIBRIUM

As was mentioned above, melt polymerization seems to lead to a complication of the simple melting scheme. Based on the analysis of experimental data on equilibria between olivine and liquids of mafic and ultramafic composition from the viewpoint of the ion model, Herzberg [22] considered the reaction

$$2(Mg^{2+})_L + (SiO_4^{4-})_L = (Mg_2SiO_4)_L \qquad (11)$$

and arrived at the conclusion that an increase in the SiO_2 concentration in the melt tends to suppress the activity of $(SiO_4^{4-})_L$ groups. However, melt polymerization is not a gradual process and begins as soon as a limiting value of Si/O ~ 0.29 is achieved. At lower values of this ratio, the melt is completely depolymerized. Proceeding from this, we consider the crystallization of magnesian olivine from ultramafic and mafic liquids (which are the least polymerized) as an illustrative example in the context of quantitatively evaluating the dilution effect. The olivine–melt equilibrium in anhydrous environments was examined by many researchers [2–5, 22–25]. The approaches proposed can be subdivided into two groups. One of them comprises empirical polynomial dependencies of the distribution coefficients of components between olivine and melt as functions of temperature, pressure, and the mole fractions of other components [24, 25]. The other, most widely used approach treats olivine crystallization in terms of the constant of a reaction between oxide components of the melt and the crystallizing magnesian or ferrous end members, similarly to reaction (2) [2–5, 22, 23]. The activities of components in the reaction constant expressions are taken to be equal to their mole fractions. The temperature and pressure functions of the reaction constants are therewith expressed as simple dependences analogous to Eq. (4). To calculate the mole fractions of melt components, the usual scheme was used [3, 4, 22–25] without subdividing components into groups in accordance with their supposed structural positions. Nielsen ad Dungan [5] proposed to calculate the cationic fractions of the components based on the two-site model for the melt structure, in which fractions are calculated separately for network-forming (SiO_2, $NaAlO_2$, and $KAlO_2$) and network-modifying (TiO_2, $AlO_{1.5}$, MgO, FeO, $FeO_{1.5}$, CaO, and MgO) components. This approach makes it possible to significantly reduce the dependence of the equilibrium constants on the composition. Also, to enhance the correlation dependencies of the equilibrium constants on temperature, the Nielsen and Dungan approach was supplemented with the use of the Al/Si ratio as a "measure" of the compositional effect [2].

It was difficult to apply the obtained temperature dependences of olivine composition on the melt composition to natural magmas because of the unknown effect of water on this equilibrium. In spite of the ultimate significance of estimates of the physicochemical conditions under which a broad spectrum of olivine-bearing volcanic rocks is produced, the use of these estimates is virtually meaningless because magmas containing no water at all do not exist and even small additions of water notably suppress the liquidus temperatures. At the same time, the dependence of the temperature of the olivine–melt equilibrium on H_2O pressure or concentration provides a potential possibility of estimating the water regime in magmas if the temperature is estimated independently.

The approaches proposed over the past few years make it possible to take into account the effect of water on the crystallization temperature of olivine. The method proposed in [16] was already mentioned above. Based on the statistical treatment of experimental data, Danyushevsky *et al.* [13] derived an equation for the difference between the calculated olivine crystallization temperatures for anhydrous conditions and the temperatures of olivine crystallization in experiments in the presence of water as a function of the water concentration in the melts. An analogous approach was recently utilized in [26] to evaluate the effect of water on the decrease in the olivine liquidus temperature. The equation thus obtained has the form

$$\Delta T_L^{Ol} = 74.403(H_2O, \text{ wt}\%)^{0.352}.$$

The influence of melt and olivine compositions on the decrease in the liquidus temperature in the presence of water is ignored in the aforementioned papers.

Sisson and Grove [15] utilized experimental data to derive the following dependence of the constant of equilibrium between the magnesian end member of olivine in water-free and water-bearing basaltic melts on temperature (K) and pressure (bar):

$$K = (X_{Mg}^{Ol})/(X_{Mg}^{L})(X_{Si}^{L})^{0.5}, \qquad (12)$$

$$\log K = 4129/T - 2.082 + 0.0146(P-1)/T, \qquad (13)$$

where X_{Mg}^{Ol} is the MgO mole fraction in olivine and X_{Mg}^{L} and X_{Si}^{L} are the fractions of the one-cation oxides (with Al presented in the form of $NaAlO_2$, $KAlO_2$, and $CaAl_2O_4$). Water was involved in the calculations in the form of $HO_{0.5}$.

Derivation of an Equation for Olivine Crystallization

In order to quantitatively characterize the effect of melt dilution with water and principally evaluate the feasibility of the approach proposed above, we limited ourselves to the analysis of the equilibrium participated by the magnesian olivine end member alone, which enabled us not to consider the redox state of the melts.

With this purpose, we used the olivine–melt equilibrium described by the reaction

$$MgO^L + 1/2SiO_2^L = MgSi_{0.5}O_2^{Ol}. \qquad (14)$$

To calculate the parameters A, B, and C in Eq. (14), for the equilibrium constant of this reaction (expression (12)), we used the equation for the liquidus of pure forsterite under dry conditions [27]

$$T(K) = 2163 + 0.00477(P-1), \ (P - \text{bar}) \qquad (15)$$

and the estimated enthalpy of its crystallization $\Delta H_{(12)} = -208.2$ cal/g [20, p. 173]. For pure forsterite and its water-free melt, $X_{MgSi_{0.5}O_2}^{Ol} = 1$, $X_{MgO}^{L} = 2/3$, and $X_{SiO_2}^{L} = 1/3$; $\ln K_0 = 0.9548$. Equation (4) can be transformed into a form analogous to Eq. (15):

$$T = \frac{A}{0.9548 - B} + \frac{C}{0.9548 - B}(P-1). \qquad (16)$$

Then, from the equality of the respective coefficients of Eqs. (15) and (16) and the relation $A = -\Delta H_{\text{Eq. (14)}}/R$, where R is the gas constant, we obtain $A = 7371$ (grad), $B = -2.453$, and $C = 0.0162$ (grad/bar). Substituting these values into Eq. (10), we derive the expression for equilibrium (14)

$$T = \frac{7371 + 0.0162(P-1)}{\ln K_0 + 2.453 + 1.5\ln[1 + 100C_w/(100 - C_w)Wn_0]}, \qquad (17)$$

which can be used to evaluate the crystallization temperature of olivine from water-bearing and dry melts.

Evaluation of the Dilution Effect

In order to qualitatively evaluate the effect of water on the decrease in the liquidus temperatures by Eq. (17), we utilized a diversity of experimental data. The simplest way is to use Eq. (17) to calculate the liquidus of the rock, because this approach makes it possible to bypass the problem of determining the equilibrium composition of the melt (if the insignificant compositional changes during the experiments are ignored). The situation with olivine is simplified by the fact that its composition is determined by the composition of the rock melt only and is virtually constant along the liquidus, because the Mg and Fe partition coefficients between olivine and melt weakly depend on temperature and pressure [3]. In fact, it is sufficient to know the liquidus temperature at 1 atm to calculate T_L at a given pressure and water concentration in the melt.

First of all, this estimation was carried out for the melting temperature of pure forsterite under water-saturated conditions (Fig. 3). The position of the water-saturated liquidus for forsterite at 10–30 kbar was constrained experimentally in [28], and the water solubility and liquidus temperature at 20 and 30 kbar was evaluated in [19, 29]. The calculations were carried out by Eq. (17) with the assumptions that all water contained

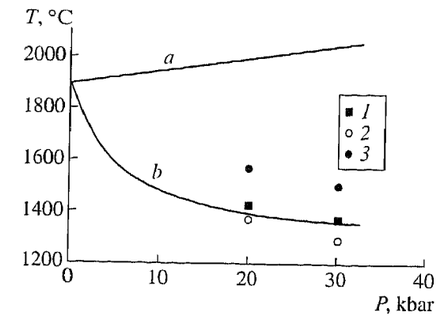

Fig. 3. Melting curves of forsterite, experimental data: (*a*) dry conditions [27], (*b*) saturation with H_2O [28]. Symbols show the forsterite liquidus at 20 and 30 kbar: (*1*) experimental data [19, 29], (*2*, *3*) calculations by Eq. (17) based on data on water solubility [19, 29] under the assumption that water is contained in the melt in the hydroxyl and molecular modes, respectively.

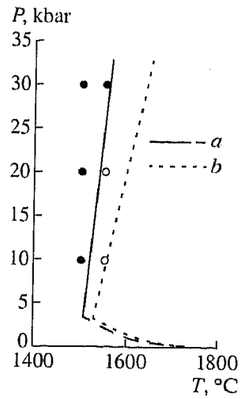

Fig. 4. Peridotite liquidus with 5.73% H_2O: (*a*) experimental data [30], (*b*) calculation. The calculation was conducted for hydroxyl water in the melt. Circles show the conditions and phase composition during the experiments: open circles correspond to the melt, solid circles show melt with olivine crystals.

in the melt is (1) in the form of hydroxyl ($W = 9.01$) or (2) in the molecular form ($W = 18.02$). As can be seen from the diagram, the experimental liquidus temperatures plot between the values calculated for different modes of water speciation, and the liquidus temperature at 20 kbar calculated for the hydroxyl mode of water in the melt is in good agreement with the experimental data. In this situation, the diluting effect of water dissolved in the melt on a decrease in melting temperature is 600°C.

Natural peridotite was studied experimentally in [30] under pressures of 10–30 kbar and a constant water concentration of 5.73%, which corresponds to under-

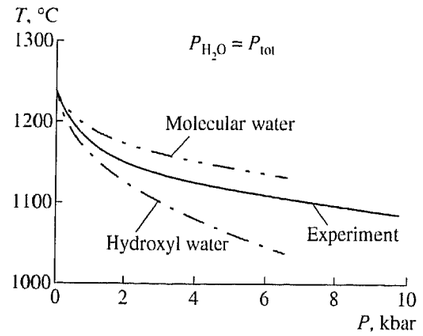

Fig. 5. Liquidus of water-saturated olivine tholeiite: experimental data [31] and calculations by Eq. (17) for different water speciation in the melt.

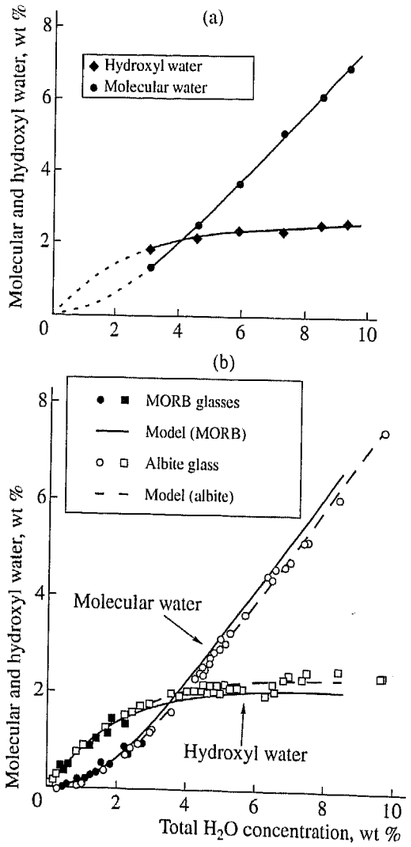

Fig. 6. (a) Distribution of water species calculated for the liquidus of olivine tholeiite (see text); (b) experimentally determined concentrations of molecular and hydroxyl water and corresponding curves, calculated by the E. Stolper model for albite and MORB [12].

saturation with water. Figure 4 presents the results of near-liquidus experiments and the stability curve for olivine, which is a liquidus phase of peridotite under these conditions. The figure also shows a calculated curve of olivine stability. Since there are no data on olivine composition in the experimental products, it was calculated from the composition of the rock and the partition coefficient [3]. The calculated temperatures are slightly higher than the experimental values perhaps owing to experimental inaccuracies such as the contamination of the thermocouples, as was noted in [30]. At the same time, the decrease in the melting temperature calculated for the hydroxyl mode of water occurrence in the melt satisfactorily fits the experimental data. Notable deviations occur only under pressures in excess of 20 kbar.

As another natural composition at which liquidus olivine is stable, we chose the olivine tholeiite Kilauea-1921, which was studied experimentally by Yoder and Tilley under water-saturated conditions [31]. Reliable information is of crucial importance for the quantitative estimation of the water effect on the melting temperatures of minerals based on the water solubility in the melt. As such we used the data of experiments on basalts at 1100°C and pressures in the range of 1–6 kbar [32]. Figure 5 shows the experimentally constrained and calculated liquidi of olivine tholeiite under water-saturated conditions. The experimental temperatures fall between the theoretical values calculated under the assumptions of fully molecular and fully hydroxyl modes of water occurrence in the melt.

It follows that the ideal model for the behavior of dissolved water particles in melt is able to quantitatively explain the decrease in the olivine melting temperature with water addition. When the calculations are carried out for the molecular mode of dissolved water particles, the needed effect cannot be achieved, while calculations for the hydroxyl mode usually result in a somewhat overestimated effect compared with experimental data. Our results are in good agreement with experimental data on the simultaneous occurrence of two water forms in silicate melts [11, 12, 33]. Equation (17) satisfactorily reproduces the shape of the P–T curve.

In order to adequately fit experimental data, we propose to use a formal value of effective water concentration (C_{ef}, wt %) instead of C_w in Eq. (17), with C_{ef} understood as a water concentration that provides a number of water particles in the melt ($n_w = C_w/W$) that actually occurs in the melt at a given water concentration (C_w) with regard for the hydroxyl (C_{hyd}) and molecular (C_{mol}) modes at a chosen form of W (9.01 or 18.02) in Eq. (18). At $W = 9.01$,

$$C_w = C_{hyd} + C_{mol}, \quad (18)$$

$$C_{ef} = C_{hyd} + 0.5C_{mol}. \quad (19)$$

Assuming $T_{calcd} = T_{exp}$ for the liquidus of Kilauea-1921 olivine tholeiite (Fig. 5), we calculated C_{hyd} and

C_{mol} from Eqs. (17)–(19) (Table 2). The values thus obtained are shown in a C_w vs. C_{hyd}, C_{mol} plot with an extrapolation to the zero value (Fig. 6a). For comparison, Fig. 6b demonstrates an analogous plot borrowed from [12] and based on experimental data on the water speciation in chill glasses of basaltic and albitic composition. In spite of the schematic character of these calculations, both plots are obviously similar.

The liquidus curves presented above (Fig. 3–5) were drawn under the assumption that the melt contained water in the form of only one species. Since the calculated temperatures depend on the assumed mode of water species, changes in the proportion of these species in the melt should affect the configuration of the calculated melting curve. As can be seen from Figs. 5 and 6, the calculated and experimental data are in good agreement. However, the region with low water concentration is characterized by a change in the predominant water species (from the hydroxyl to molecular), and the experimental curve is extrapolated. The effect of this change on the configuration of the tholeiite melting curve (Fig. 5) was estimated based on experimental data on the distribution of water species at its low concentrations in the melt (Fig. 6b). This effect is expressed in the appearance of a small bend ($d^2T_l/dP^2 = 0$) in the tholeiite liquidus in the region of very low pressures (<0.3 kbar). However, the water solubility in this region can attain petrologically significant values of 1.5–2%, which should be taken into account when an empirical solubility equation is derived.

Thus, a change in the curvature of experimental T–P and T–H_2O plots (such as curve d in Fig. 1) for various systems suggests a change in the speciation of dissolved water in the melts.

Table 2. Calculated concentrations of hydroxyl and molecular water in melt for olivine tholeiite

Water concentration in melt, wt %	P, kbar					
	1.034	2.0	3.0	4.0	5.34	6.07
Total	3.09	4.59	5.93	7.30	8.51	9.37
Hydroxyl	1.77	2.18	2.32	2.29	2.67	2.55
Molecular	1.32	2.41	3.61	5.01	5.84	6.82

Note: The total water concentration is after [32].

Table 3. Average deviations of the calculated temperature for the olivine–melt equilibrium from the experimentally determined values [14, 15]

Calculation method for water speciation in melt	1	2	3	4	5	6
	ΔT, °C					
I	25	16	20	15	22	16*
II	43	32	39	31	41	21*

* Without one experiment with a very high deficit (13.3 wt %) of the analytical total for a chill glass, apparently exceeding water solubility at $P = 2$ kbar. $\Delta T = |T_{calcd} - T_{exp}|$, average of data on 29 experiments; (*1–6*) are calculation variants of water solubility (see text); (**I**) calculation for completely hydroxyl water; (**II**) calculation for effective water concentration (see text).

The Olivine–Water-Bearing Melt as a Geothermometer

The constants obtained above for the melting of forsterite make it possible to utilize Eq. (17) as a geothermometer. Note that they were derived without statistical calibration of the equations against experimental data. To assay the principal acceptability of this method, we used experimental data on the melting of basaltic compositions under water-saturation conditions [14, 15], which were used by the authors of these papers, along with the results of other experiments with melting in dry and water-bearing environments, as the basis for the calibration of the olivine geothermometer [15].

In order to calculate the equilibrium temperatures for olivine–melt pairs, we used a variety of techniques for estimating the water concentrations in melts in equilibrium with the olivine:

(1) the model of Silver and Stolper with the use of the computer program in [12]; [3]

(2) the Burnham model [9];

(3) the modified Burnham model [10];

(4) the model of Al'meev and Ariskin [16];

(5) the Moore *et al.* model [34]; and

(6) calculations as the deficit of the analytical totals of microprobe analyses.

The calculations were carried out by a computer program devised for this purpose. Since the calculations of water concentrations by methods (2)–(4) require knowledge of the temperature, the program involved an iteration procedure that enabled determining the temperature accurate to 0.5°C. The calculations were conducted in two variants. In one of them, it was assumed that all water is contained in the melt in the form of hydroxyl. In the other variant, which was aimed at approximately evaluating the probable presence of different water species in the melt, their concentrations were calculated in compliance with the Silver and Stolper model. The concentration proportions of molecular and hydroxyl water calculated in this manner

[3] This program, translated into FORTRAN, was kindly provided for us by R.R. Al'meev.

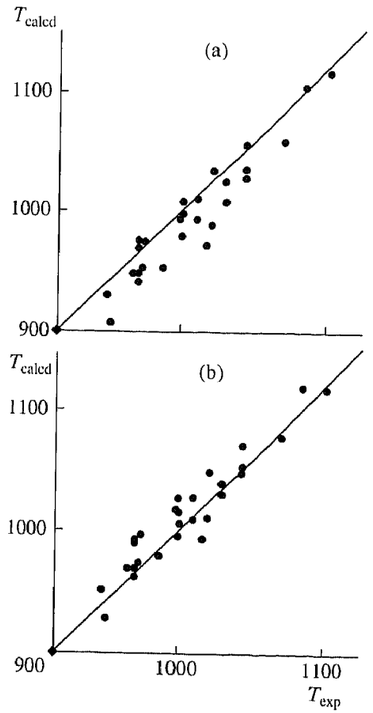

Fig. 7. Experimental ([14, 15]) and calculated [by Eq. (17), $W = 9.01$] temperatures of the olivine–melt equilibrium. The water concentration in the melt was determined as the deficit of the analytical totals of microprobe analyses. (a) Mole fractions of components calculated for one-cation basis; (b) same, with Al in the form of $NaAlO_2$ and $KAlO_2$.

were also assumed for other models of water solubility. After this, the effective water concentration was calculated with regard for relations (17)–(19) and, then, the temperature of the olivine–melt equilibrium. The average deviations of the calculated temperatures from experimental values in different variants of the calculations are listed in Table 3.

In general, the calculated figures are in good agreement with the experimental data when the calculations are carried out for hydroxyl water in variants (2), (4), and (6) ($\Delta T_{average}$ = 15–16°C). This implies that Eq. (17) can be used as a geothermometer for olivine equilibria in water-bearing melts or as a tool for determining the concentration of water, if one of this parameters can be evaluated independently. The estimation of the water concentrations seems to be more reliable at low concentration values and involve significant errors closer to the limiting water solubility values because of a weaker dependence of the melting temperature on the water concentration ($|dT_L/dC_w| \longrightarrow 0$). The calculated temperatures also significantly depend on the reliability of the water concentrations in the melts estimated by different methods. Note the good compatibility between the calculated and experimental temperatures when the water concentrations were derived from the analytical totals of microprobe analyses. The calculation models of variants (1)–(5) mostly show temperature overestimates, while calculations from the analytical totals, conversely, yield underestimates (Fig. 7a). Hence, it can be hypothesized that the calculation models underestimate the actual water concentrations, and the latter variant provides slight overestimates. At the same time, our analysis demonstrates that an increase in the alkalinity of the melts is associated with systematic deviations of the calculated temperatures toward underestimates. This can be interpreted as an indication that the melt contains alkaline complexes, as was proposed in [15], such as $NaAlO_2$, $KAlO_2$, and $CaAl_2O_4$. Therewith the supposed number of particles in the melt decreases, which results, according to (5), (12), and (17), in an increase in the calculated temperatures.

Temperature estimates by Eq. (17) with the calculation of cation fractions in the melt according to the scheme adopted in [15] result in significant overestimates of the calculated temperatures relative to the experimental values and a significantly deteriorated quality of the results. The best agreement between the calculated and experimental temperatures ($\Delta T_{average}$ = 12°C) is achieved when Al is incorporated only in $NaAlO_2$ and $KAlO_2$ and the concentrations of water (in the form of OH groups) are calculated from analytical totals (Fig. 7b).

CONCLUSIONS

As can be seen from the materials presented above, the analysis of equilibria in silicate melts from the viewpoint of the ideal model can in principle account for both the water effect on the morphology of the melting curves for anhydrous silicates and the needed quantitative effect of a decrease in the melting temperature in the presence of water. This makes it possible to utilize such an approach for petrological evaluations in the absence of required experimental information, as well as for the thermodynamic analysis of equilibria in melts. In particular, this approach enables a more natural interpolating between the temperatures of the dry and water-saturated melting of minerals in the theoretical modeling of water-bearing magma differentiation, in contrast to the linear dependence assumed in [2, 16].

A difficulty in the application of this analysis is related to the dependence of the structure of a melt on its composition and, correspondingly, the complication of the melt speciation, as well as the redistribution of the dissolved water species as a function of the *P–T* parameters. This causes the necessity of selecting the equilibrium constants of reactions depending on the specified spectrum of natural melts in terms of silicity and alkalinity [4, 22] and the representation of the

silicate melts in the form of two independent sublattices [5].

An avenue for further research as a continuation and development of this approach can be the selection and analysis of probable melting reactions of other minerals. Conceivably, a combination of reactions can make it possible to take into account the effect of the melt composition and structural changes in it at unchanging coefficients of the *P–T* functions of the reaction constants. From the viewpoint of our conclusions, it seems to be promising to conduct the coupled experimental study of the crystallization temperatures and the structures of water-bearing melts, in particular, the distribution of water species along the liquidus in the *P–T* and *T*–H_2O space.

ACKNOWLEDGMENTS

The author thanks A.A. Ariskin, R.R. Al'meev, and O.A. Lukanin (Vernadsky Institute of Geochemistry and Analytical Chemistry, Russian Academy of Sciences) for help in this research and discussion of its results. This study was supported by the Russian Foundation for Basic Research, project nos. 96-05-65992 and 99-05-65495

REFERENCES

1. Ghiorso, M.S. and Sack, R.O., Chemical Mass Transfer in Magmatic Processes: IV. A Revised and Internally Consistent Thermodynamic Model for the Interpolation and Extrapolation of Liquid–Solid Equilibria in Magmatic Systems at Elevated Temperatures and Pressures, *Contrib. Mineral. Petrol.*, 1995, vol. 119, pp. 197–212.
2. Ariskin, A.A. and Barmina, G.S., *Modelirovanie fazovykh ravnovesii pri kristallizatsii bazal'tovykh magm* (Modeling of Phase Equilibria for Crystallization of Basaltic Magmas), Moscow: Nauka, 2000.
3. Roeder, P.L. and Emslie, R.F., Olivine–Liquid Equilibrium, *Contrib. Mineral. Petrol.*, 1970, vol. 29, no. 4, pp. 275–289.
4. Longhi, J., Walker, D., and Hays, J.F., The Distribution of Fe and Mg between Olivine and Lunar Basaltic Liquid, *Geochim. Cosmochim. Acta*, 1978, vol. 42, no. 10, pp. 1545–1558.
5. Nielsen, R.L. and Dungan, M.A., Low Pressure Mineral–Melt Equilibria in Natural Anhydrous Mafic Systems, *Contrib. Mineral. Petrol.*, 1983, vol. 84, no. 4, pp. 310–326.
6. Kadik, A.A., Lebedev, E.B., and Khitarov, N.I., *Voda v magmaticheskikh rasplavakh* (Water in Magmas), Moscow: Nauka, 1971.
7. Anfilogov, V.N. and Bobylev, I.B., Thermodynamic Analysis of Water Solution in Silicic Melts, *Geokhimiya*, 1985, no. 9, pp. 1277–1285.
8. Epel'baum, M.B. and Chekhmir, A.S., On a Model of Silicic Melt–Water Interaction, in *Ocherki fiziko-khimicheskoi petrologii* (Sketches in Physicochemical Petrology), 1991, no. 16, pp. 15–27.
9. Burnham, C.W., Volatiles in Magmas, in *The Evolution of the Igneous Rocks*, Yoder, H.S., Jr., Ed., Princeton: Princeton Univ. Press, NJ, 1979.
10. Burnham, C.W., Development of the Burnham Model for Prediction of the H_2O Solubility in Magmas, in *Reviews in Mineralogy*, 1994, vol. 30: *Volatiles in Magmas*, pp. 187–230.
11. Stolper, E., The Speciation of Water in Silicate Melts, *Geochim. Cosmochim. Acta*, 1982, vol. 46, no. 12, pp. 2609–2620.
12. Holloway, J.R. and Blank, J.G., Application of Experimental Results to C–O–H Species in Natural Melts, in *Reviews in Mineralogy*, 1994, vol. 30: *Volatiles in Magmas*, pp. 187–230.
13. Danyushevskii, L.V., Sobolev, A.V., and Kononkova, N.N., The Ability of Analytical Methods for Mineral-enclosed Melt Inclusions for Studying Water-bearing Primitive Mantle Melts: Evidence from Boninites of the Tonga Trench, *Geokhimiya*, 1991, no. 12, pp. 1711–1723.
14. Sisson, T.W. and Grove, T.L., Experimental Investigations of the Role of H_2O in Calc-alkaline Differentiation and Subduction Zone Magmatism, *Contrib. Mineral. Petrol.*, 1993, vol. 113, no. 2, pp. 143–166.
15. Sisson, T.W. and Grove, T.L., Temperatures and H_2O Contents of Low-MgO High-Alumina Basalts, *Contrib. Mineral. Petrol.*, 1993, vol. 113, no. 2, pp. 167–184.
16. Al'meev, R.R. and Ariskin, A.A., Computer Modeling of Melt–Mineral Equilibria in Water-containing Basaltic System, *Geokhimiya*, 1996, no. 7, pp. 624–636.
17. Kadik, A.A., Maksimov, A.P., and Ivanov, B.V., *Fiziko-khimicheskie usloviya kristallizatsii i genezis andezitov (na primere Klyuchevskoi gruppy vulkanov)* (Physicochemical Conditions of Crystallization and the Genesis of Andesites with Reference to the Klyuchevskaya Group of Volcanoes), Moscow: Nauka, 1986.
18. Stern, C.R., Huang, W.-L., and Wylie, P.J., Basalt–Andesite–Rhyolite–H_2O: Crystallization Intervals with Excess H_2O and H_2O-undersaturated Liquidus Surfaces to 35 Kilobars, with Implications for Magma Genesis, *Earth Planet. Sci. Lett.*, 1975, vol. 28, no. 2, pp. 189–196.
19. Hodges, F.N., The Solubility of H_2O in Silicate Melts, *Carnegie Inst. Year Book* (Washington), 1974, vol. 73, pp. 251–255.
20. Yoder, H.S., *Generation of Basaltic Magma*, Washington, 1976. Translated under the title *Obrazovanie bazal'tovoi magmy*, Moscow: Mir, 1979.
21. Naumov, G.B., Ryzhenko, B.N., and Khodakovskii, I.L., *Spravochnik termodinamicheskikh velichin* (Thermodynamic Handbook), Moscow: Atomizdat, 1971.
22. Herzberg, C.T., The Solubility of Olivine in Basaltic Liquids: An Ionic Model, *Geochim. Cosmochim. Acta*, 1979, vol. 43, no. 8, pp. 1241–1251.
23. Leeman, W.P., Distribution of Mg^{2+} between Olivine and Silicate Melt, and Its Implications Regarding Melt Structure, *Geochim. Cosmochim. Acta*, 1978, vol. 42, no. 6, pp. 789–800.
24. Ford, C.E., Russel, D.G., Craven, J.A., and Fisk, M.R., Olivine–Liquid Equilibria: Temperature, Pressure, and Composition Dependence of Crystal–Liquid Cation Par-

tition Coefficients for Mg, Fe^{2+}, Ca, and Mn, *J. Petrol.*, 1983, vol. 24, no. 3, pp. 256–265.

25. Glazner, A.F., Activities of Olivine and Plagioclase Components in Silicate Melts and Their Application to Geothermometry, *Contrib. Mineral. Petrol.*, 1984, vol. 88, no. 3, pp. 260–268.

26. Falloon, T.J. and Danyushevskii, L.V., Melting of Refractory Mantle at 1.5 and 2 GPa under H_2O-undersaturated Conditions: Implications for the Petrogenesis of High-Ca Boninites, *J. Petrol.*, 2000, vol. 41, no. 2, pp. 257–283.

27. Davis, B.T.C. and England, J.L., The Melting of Forsterite up to 50 Kilobars, *J. Geophys. Res.*, 1964, vol. 69, no. 6, pp. 1113–1116.

28. Kushiro, I. and Yoder, H.S., Jr., Melting of Forsterite and Enstatite at High Pressures under Hydrous Conditions, *Carnegie Inst. Year Book* (Washington), 1968, vol. 67, pp. 153–158.

29. Hodges, F.N., Solubility of H_2O in Forsterite Melt at 20 kbar, *Carnegie Inst. Year Book* (Washington), 1973, vol. 72, pp. 495–497.

30. Millhollen, G.L., Irving, A.J., and Wyllie, P.J., Melting Interval of Peridotite with 5.7 Percent Water to 30 Kilobars, *J. Geol.*, 1974, vol. 82, no. 5, pp. 575–587.

31. Yoder, H.S., Jr. and Tilley, C.E., Origin of Basalt Magmas: An Experimental Study of Natural and Synthetic Rock Systems, *J. Petrol.*, 1962, vol. 3, pp. 342–532.

32. Hamilton, D.L., Burnham, C.W., and Osborn, E.F., The Solubility of Water and Effects of Oxygen Fugacity and Water Content on Crystallization in Mafic Magmas, *J. Petrol.*, 1964, vol. 5, pp. 21–39.

33. Silver, L.A., Ihinger, P.D., and Stolper, E., The Influence of Bulk Composition on the Speciation of Water in Silicate Glasses, *Contrib. Mineral. Petrol.*, 1990, vol. 104, no. 2, pp. 142–162.

34. Moore, G., Vennemann, T., and Carmichael, I.S.E., An Empirical Model for the Solubility of H_2O in Magmas to 3 Kilobars, *Am. Mineral.*, 1998, vol. 83, pp. 36–42.